Pharmacogenomics and Personalized Medicine

Dovepress

open access to scientific and medical research

Open Access Full Text Article

ORIGINAL RESEARCH

The Correlation of Centromere Protein Q with Diagnosis and Prognosis in Hepatocellular Carcinoma

Kun He[1,2,*], Meng-yi Xie[1,2,*], Xiao-jin Gao[1,2,*], Hao Wang[1,2], Jing-dong Li[1,2]

[1]Institute of Hepatobiliary, Pancreatic and Intestinal Diseases, North Sichuan Medical College, Nanchong, Sichuan, People's Republic of China; [2]Department of Hepatobiliary and Pancreatic Surgery, Affiliated Hospital of North Sichuan Medical College, Nanchong, Sichuan, People's Republic of China

*These authors contributed equally to this work

Correspondence: Jing-dong Li, Email lijingdong358@nsmc.edu.cn

Introduction: Hepatocellular carcinoma (HCC) is one of the major types of liver cancer. Previous studies have shown that the centromere protein family is associated with malignant biological behaviors such as HCC proliferation. As a member of the centromere protein family, centromere protein Q (CENPQ) is closely associated with immunotherapy and immune cell infiltration in various tumors. However, the role and mechanism of CENPQ in HCC remain unclear.

Methods: Multiple public databases and RT-qPCR were used to study the expression of CENPQ in HCC. Based on TCGA data, the correlation between CENPQ and clinicopathological characteristics and prognosis of HCC patients was analyzed, and its diagnostic value was evaluated. The potential biological functions of CENPQ in HCC were explored by functional enrichment analysis of differentially expressed genes. The distribution of tumor-infiltrating immune cell types was assessed using single-sample GSEA, and immune checkpoint gene expression was analyzed using Spearman correlation. Subsequently, loss-of-function experiments were performed to determine the function of CENPQ on the cell cycle and proliferation of HCC cells in vitro.

Results: CENPQ was found highly expressed in HCC and correlated with weight, BMI, age, AFP, T stage, pathologic stage, histologic grade, and prothrombin time (all $p < 0.05$). ROC and Kaplan-Meier analyses indicated that CENPQ may be potentially used as a diagnostic marker for HCC (AUC = 0.881), and its upregulation is associated with decreased OS ($p = 0.002$), DSS ($p < 0.001$), and PFI ($p = 0.002$). Functional enrichment analysis revealed an association of CENPQ with biological processes such as immune cell infiltration, cell cycle, and hippo-merlin signaling deregulation in HCC. Furthermore, knockdown of CENPQ manifested in HCC cells with G0/1 phase cycle arrest and decreased proliferative capacity.

Conclusion: CENPQ expression was higher in HCC tissues than in normal liver tissues. It was significantly associated with poor prognosis, immune cell infiltration, cell cycle, and proliferation. Therefore, CENPQ may become a promising prognostic biomarker for HCC patients.

Keywords: centromere protein Q, biomarker, immune infiltration, cell cycle, hepatocellular carcinoma

Introduction

Liver cancer is one of the most frequent malignant tumors globally and has a poor prognosis and high mortality. Its most frequent histological subtype is hepatocellular carcinoma (HCC), which accounts for ~90% of cases, whereas cholangiocarcinoma and mixed subtypes account for the remaining ~10%.[1] Current therapeutic options for HCC include liver resection, liver transplantation, thermal tumor ablation, radiation therapy, transarterial chemoembolization (TACE), selective internal radiotherapy (SIRT), chemotherapy, and immunotherapy.[2] Surgical resection is the preferred treatment for HCC patients to achieve good long-term survival. Due to the lack of characteristic clinical symptoms and rapid advancement of early-stage HCC, 70–80% of patients are in an advanced stage when detected and thus miss the opportunity for surgery.[3] Patients with advanced HCC may benefit from immunotherapy, and several immunomodulating

Received: 1 February 2024
Accepted: 18 May 2024
Published: 27 May 2024

drugs have been utilized to treat HCC.[4–6] The effectiveness of immunotherapy for cancer patients is influenced by the abundance and phenotypic distribution of immune cells in the tumor microenvironment, as well as by tumor stage. Despite recent improvements in the diagnosis and treatment of HCC, the overall prognosis of patients remains poor because of the challenging concerns of recurrence, metastasis, and tumor immunotolerance. The 5-year survival rate for advanced HCC is estimated to be less than 12%,[7] and ranges from 7–20% for cholangiocellular carcinoma.[8] Therefore, there is an urgent need to identify new therapeutic targets and better markers for early detection, treatment, and prognostic monitoring of HCC.

Centromere proteins (CENPs) are crucial proteins involved in cell division and proliferation as well as the structure and function of centromeres. Abnormal expression and localization of CENPs can lead to chromosome segregation disorders and the formation of aneuploidy, which is one of the major causes of tumors.[9] The importance of CENPs in oncogenesis has been demonstrated by a series of earlier studies. For example, overexpression of CENPO is associated with the progression of bladder cancer,[10] colorectal cancer,[11] and gastric cancer.[12] Meanwhile, a series of centromere protein members such as CENPE,[13] CENPF,[14] CENPH,[15] CENPO,[16] and CENPW[17] has also been found to be associated with the development of HCC. Centromere protein Q (CENPQ), also known as chromosome 6 open reading frame 139, is a 268 amino acid, ~31 kDa protein encoded by a 9-exon gene located at chromosome 6p12.3. Interestingly, CENPQ can be regulated by LINC01857 and miR-2052 to inhibit metastasis and angiogenesis in breast cancer cells.[18] However, in HCC the function of CENPQ and the impact of its dysregulated expression remain unclear.

In the present study, differential expression of CENPQ mRNA and protein in HCC was confirmed upon examination of various cancer databases and validated in clinical HCC samples. In addition, the relationship between CENPQ expression and clinicopathological features and patient prognosis, as well as the potential utility of CENPQ as a diagnostic marker, were investigated. Moreover, the potential regulatory mechanism of CENPQ in HCC was initially explored, and the relationship between CENPQ expression and both immune cell infiltration and immune checkpoint expression in HCC was analyzed. Lastly, experiments were performed to verify the expression of CENPQ in HCC cell lines and to detect its proliferation and cycle changes in vitro after knocking down CENPQ in HCC cell lines. We thus provide a first account of CENPQ dysregulation in HCC, which we hope will encourage further research to improve treatment options and patient outcomes.

Materials and Methods

Ethical Statement

All human tissue specimens used in our studies were collected and classified in accordance with the principles of the Helsinki Declaration of the World Medical Association. The Ethics Committee of the Affiliated Hospital of North Sichuan Medical College approved the study protocol (Approval No.2022ER464-1). Written informed consent was obtained from patients before obtaining tissue samples.

Data Sources and Processing

RNA-sequencing profiles from pan-cancer and normal tissues were mined from the Genotype-Tissue Expression (GTEx) and The Cancer Genome Atlas (TCGA) databases. RNA-sequencing profiles of liver cancer cells were obtained from the Depmap database. Clinical information and RNA-seq corresponding to 374 HCC patients were also downloaded from the TCGA database. Microarray datasets for liver cancer (GSE98383, GSE107170)[19] were downloaded from the Gene Expression Omnibus (GEO) database to validate the expression of CENPQ mRNA in HCC. In addition, we obtained immunohistochemical staining (IHC) images from the Human Protein Atlas (HPA) database to assess CENPQ protein expression in HCC.[20] All IHC images were analyzed by computing mean integrated optical density (IOD) values with Image-Pro Plus software. Correlation analyses between RNA-seq profiles of 374 HCC cases obtained from TCGA and corresponding clinical information were conducted using R software and logistic regression.

Analysis of the Diagnostic and Prognostic Value of CENPQ in HCC

The diagnostic and prognostic value of CENPQ in HCC was estimated based on RNA-seq data and corresponding clinical information from 374 HCC samples and 50 normal tissue samples obtained from TCGA. Diagnostic performance was assessed using the R package "pROC" to draw receiver operating characteristic (ROC) curves and calculate the area under the curve (AUC). Cases were separated into high and low CENPQ mRNA expression groups according to the median expression value of CENPQ, and survival curves were plotted with the R package "Survival" to compare prognosis measures (OS, DSS, and PFI) for both groups.

Identification and Functional Enrichment Analysis of Differentially Expressed Genes (DEGs)

According to the median expression value of CENPQ mRNA, based on RNA-seq data from TCGA, DEGs in the high and low CENPQ mRNA expression groups were identified by the R package "DESeq2"[21] Adjusted $p<0.05$ and $|\log_2 FC|>1$ were set as the thresholds for DEGs. The R package "ClusterProfiler"[22] was used to perform Gene Ontology (GO) analysis, Kyoto Gene and Genome Encyclopedia (KEGG) analysis, and Gene Set Enrichment Analysis (GSEA) on the DEGs. From MSigDB Collections, "h.all.v7.2.symbols.GMT[Hallmarks]" was selected as the reference genome for pathway analysis. Significant enrichment was defined for genes with adjusted $p < 0.05$ and false discovery rate (FDR) < 0.25.

Immune Cell Infiltration Analysis

The relationship between immune cell types and CENPQ expression in HCC was analyzed with the single sample GSEA (ssGSEA) algorithm in the R package "GSVA"[23] and evaluated by Spearman correlation. Immune cell infiltration scores for the high and low CENPQ expression groups were determined and subsequently analyzed by the Wilcoxon rank sum test. The correlation between CENPQ expression and classical immune checkpoints was also assessed by Spearman correlation.

Tissue Sample Sources

A total of 10 samples of HCC tissues and their matched paracancerous tissues were collected between June 2022 and October 2022 at the First Department of Hepatobiliary and Pancreatic Surgery of the Affiliated Hospital of North Sichuan Medical College. None of the patients had received radiotherapy, chemotherapy or immunotherapy prior to surgery. All samples were confirmed by two pathologists for diagnosis after surgery. Tissue specimens were placed in liquid nitrogen immediately after collection and then stored at −80°C prior to processing.

HCC Cell Lines and Culture Conditions

Human liver cancer HEP3B, HUH7, HEPG2, and MHCC97H cell lines were purchased from the National Collection of Authenticated Cell Cultures (Shanghai, China). HEP3B, HUH7, and MHCC97H cells were cultured in Dulbecco's Modified Eagle's Medium (DMEM) (VivaCell; Shanghai, China) containing 10% fetal bovine serum (VivaCell) and 1% penicillin-streptomycin (VivaCell). HEPG2 was cultured in Minimum Essential Medium (MEM) (VivaCell) with 10% fetal bovine serum (VivaCell) and 1% penicillin-streptomycin (VivaCell).

RNA Interference and Transfection

Three different targeting CENPQ small interfering RNAs were designed and synthesized from Shanghai Integrated Biotech Solutions Co., Ltd (IBSBIO, Shanghai, China). siCENPQ-1 (sense, 5'-GGUAGAGACCACAGAGUUAAU-3', anti-sense, 5'-UAACUCUGUGGUCUCUACCAU-3'). siCENPQ-2 (sense, 5'-GGACAAACAAAGCACACUAAC-3'; anti-sense, 5'-UAGUGUGCUUUGUUUGUCCUU-3'). siCENPQ-3 (sense, 5'-GGAAGAUUUAACUAAUGUAUC-3'; anti-sense, 5'-UACAUUAGUUAAAUCUUCCAU-3'). si-NC (sense, 5'-UUCUCCGAACGUGUCACGUTT-3';anti-sense, 5'-ACGUGACACGUUCGGAGAATT-3'). Cells were inoculated at 2×10^5 cells/well into 24-well plates for 24 h. Transfection was performed when confluency reached ~40%. According to the manufacturer's protocol, 50 nmol/L

siRNA was transfected into HUH7 and HEPG2 cells, respectively, using Lipofectamine™ 3000 (Thermo Fisher Scientific, Shanghai, China).

Reverse Transcription-Quantitative Polymerase Chain Reaction (RT-qPCR)

CENPQ mRNA expression was detected by RT-qPCR using SYBR Green PCR Kits (Vazyme Biotech, Nanjing, China). Briefly, total RNA was collected from cells or tissues using the TRIzol method. After removing genomic DNA, cDNA was synthesized using a reverse transcription kit (Vazyme, Nanjing, China) and subjected to RT-qPCR. Primer sequences (synthesized by Sangon Biotech., Shanghai, China) were: CENPQ: forward, 5'-AAACCTGGCAACCTCTGTCAAAG -3', reverse, 5'-TCTCCTCTTCTTCTTCCACCTCAC-3'; GAPDH: forward, 5'-AAGGTCATCCCTGAGCTGAA-3', reverse, 5'-TGACAAAGTGGGCGTTGAGG-3'. CENPQ gene expression results were normalized to GAPDH.

Flow Cytometry Analysis of Cell Cycle Assay

Cell cycle analysis was performed using a Cell Cycle Detection Kit (Beyotime, Shanghai, China) according to the manufacturer. Briefly, cells were washed with cold PBS and fixed in 75% pre-cooled ethanol at 4°C overnight. After removing the ethanol, cells were suspended in 500 μL of propidium iodide (Beyotime, Shanghai, China) and incubated for 30 min at 4°C, protected from light. The cells were then dispersed by vortex shaking and filtered through a nylon sieve. Next, flow cytometry (ACEA Biosciences, Hangzhou, China) was used to analyze the cell cycle.

Cell Counting Kit-8 (CCK-8) Assay

Cell viability was assessed using CCK-8 (Beyotime, Shanghai, China). Transfected HUH7 and HEPG2 cells were collected with trypsin and inoculated in 96-well plates at a density of 5×10^4 cells/mL, respectively. Incubated overnight, CCK-8 (10 μL/well) was added to each well at 0, 12, 24, 48, and 72 h. Cells were incubated at 37°C for 60 min and absorbance at 450 nm was measured using a microplate reader (BIO-RAD). The OD values were plotted on the vertical axis and time on the horizontal axis to obtain the cell growth curve. This experiment was repeated three times.

Statistical Analysis

R software (version 3.6.3) and GraphPad Prism (version 8.0) were used for statistical analysis and data visualization. The Wilcoxon rank sum test or the *t*-test were used to compare two groups. The Wilcoxon rank sum test and logistic regression were used to analyze the relationship between CENPQ and clinicopathological characteristics. The Log rank test was used for survival analysis. Correlation was determined by Spearman's r. Two-tailed $p < 0.05$ was considered significant.

Results

Clinicopathological and Demographic Characteristics of HCC Patients

Cases were excluded where clinicopathological information, prognostic data, and RNA-Seq profiles were missing. A total of 374 HCC patients (121 females and 253 males) with clinical data including gender, age, weight, BMI, AFP, ALB, prothrombin time, Child-Pugh classification, Ishak fibrosis score, TNM stage, pathological stage, residual tumor, histological grading, adjacent liver tissue inflammation, and vascular invasion were included in the analysis. Records indicated that 76.8% of patients (n = 215) had AFP ≤ 400 ng/mL, and 23.2% of patients (n = 65) had AFP > 400 ng/mL. ALB < 3.5 g/dl was recorded in 23% of patients (n = 69) and ALB ≥ 3.5 g/dl in 77% of patients (n = 231). Prothrombin time was ≤4 seconds in 70% of patients (n = 208) and >4 seconds in 30% of patients (n = 89). Child-Pugh grade distribution data informed 219 cases (90.9%) in Child-Pugh A and 22 cases (9.1%) in Child-Pugh B-C stage. On the Ishak fibrosis scale, there were 106 cases (49.3%) with scores between 0–2 and 109 cases (50.7%) with scores between 3–6. There were 278 patients (74.9%) with T1-T2 stage and 93 patients (25.1%) with T3-T4 stage. Pathologic stage distribution included 260 patients (74.3%) with stage I–II and 90 patients (25.7%) with stage III–IV. Only 5.2% of cases (18/345) had R1-R2 postoperative marginal residual tumors. Histological grades included 233 (63.1%) G1-G2 and 136 (36.9%) G3-G4 cases. Among 237 and 318 patients for which pertinent data were available, 50.2% (119 patients) and

Table 1 Clinicopathological Characteristics of HCC Patients

Characteristics		Cases	%
Gender	Female	121	32.4
	Male	253	67.6
Race	Asian	160	44.2
	Black or African American or White	202	55.8
Age (years)	≤60	177	47.5
	>60	196	52.5
Weight (kg)	≤70	184	53.2
	>70	162	46.8
Height (cm)	<170	201	58.9
	≥170	140	41.1
BMI (kg/m^2)	≤25	177	52.5
	>25	160	47.5
AFP (ng/mL)	≤400	215	76.8
	>400	65	23.2
ALB (g/dl)	<3.5	69	23
	≥3.5	231	77
Prothrombin time (sec)	≤4	208	70
	>4	89	30
Child-Pugh grade	A	219	90.9
	B and C	22	9.1
Ishak fibrosis score	0–2	106	49.3
	3–6	109	50.7
T stage	T1 and T2	278	74.9
	T3 and T4	93	25.1
N stage	N0	254	98.4
	N1	4	1.6
M stage	M0	268	98.5
	M1	4	1.5
Pathologic stage	I and II	260	74.3
	III and IV	90	25.7
Residual tumor	R0	327	94.8
	R1 and R2	18	5.2
Histologic grade	G1 and G2	233	63.1
	G3 and G4	136	36.9
Adjacent hepatic tissue inflammation	No	118	49.8
	Yes	119	50.2
Vascular invasion	No	208	65.4
	Yes	110	34.6

Abbreviations: AFP, alpha fetoprotein; ALB, albumin; BMI, body mass index.

34.6% (110 patients) had adjacent liver tissue inflammation and vascular invasion, respectively. Further detailed data are presented in Table 1.

Analysis of CENPQ mRNA and Protein Expression in HCC

Pan-cancer studies showed that CENPQ mRNA expression was upregulated in most cancers, including liver hepatocellular carcinoma (LIHC), pancreatic adenocarcinoma (PAAD), and cholangiocarcinoma (CHOL) (Figure 1A). The expression of CENPQ in various HCC cells from the Depmap database was analyzed. CENPQ mRNA was detected in most of the HCC cells, with higher expression of CENPQ in SNU387 and SNU423 cells (Figure 1B). Further analysis of a TCGA-HCC cohort (50 cases) revealed that CENPQ mRNA expression was collectively increased in HCC compared to paired paracancerous tissues ($p = 3.2e\text{-}11$; Figure 1C). Similarly, it was also elevated in 374 HCC cases compared to

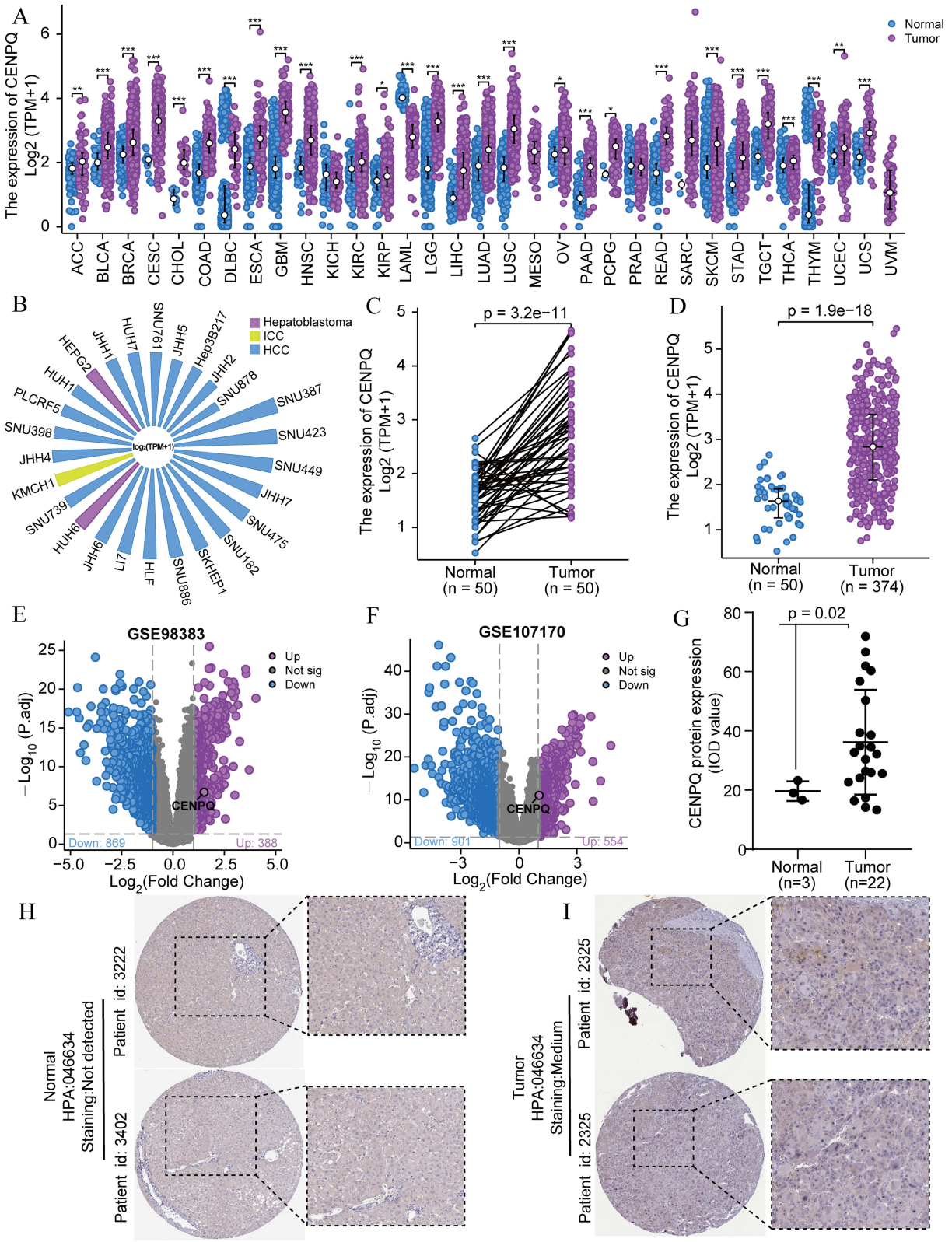

Figure 1 CENPQ expression data in hepatocellular carcinoma (HCC). (**A**) Pan-cancer analysis of CENPQ mRNA expression. (**B**) CENPQ mRNA expression in HCC cell lines. (**C**) Analysis of CENPQ mRNA expression in HCC and paired non-cancerous, adjacent tissues. (**D**) Analysis of CENPQ mRNA expression in HCC and unpaired non-cancerous, adjacent tissues. (**E**) Analysis of CENPQ mRNA expression in the GEO dataset GSE 98383. (**F**) Analysis of CENPQ mRNA expression in the GEO dataset GSE 107170. (**G**) Mean integrated optical density (IOD) values of IHC images of liver and HCC. (**H** and **I**) CENPQ protein expression images in normal and HCC. *p < 0.05, **p < 0.01, ***p < 0.001.

50 unpaired paracancerous tissues (p = 1.9*e*-18; Figure 1D). High CENPQ mRNA expression in HCC was further confirmed upon analysis on GEO HCC microarray datasets GSE98383 (Figure 1E) and GSE107170 (Figure 1F). In turn, data from HPA database indicated that CENPQ protein levels were significantly upregulated in HCC compared to normal tissue (p = 0.02; Figures 1G, H, and I). The above results thus showed that the expression of CENPQ is both at the mRNA and protein levels characteristically higher in HCC than in normal liver tissue.

Correlation of CENPQ Expression with Clinicopathological Characteristics of HCC

We further analyzed the relationship between CENPQ expression and various clinicopathological features. As shown in the violin plots in Figures 2A–H, Wilcoxon rank sum test analyses indicated that CENPQ expression was associated with weight (p = 1.8*e*-03; Figure 2A), BMI (p = 0.047; Figure 2B), age (p = 0.01; Figure 2C), AFP (p = 3.8*e*-04; Figure 2D), T stage (Figure 2E), pathologic stage (Figure 2F), histologic grade (Figure 2G), and prothrombin time (p = 0.04; Figure 2H). In addition, logistic regression analysis provided similar results, as detailed in Table 2. The above results suggest that CENPQ mRNA expression is higher in HCC patients with malignant pathological features.

Diagnostic and Prognostic Value of CENPQ in HCC

We conducted ROC analysis to assess the feasibility of using CENPQ as a diagnostic indicator of HCC. Results indicated that CENPQ had good diagnostic ability for HCC (area under the ROC curve, AUC = 0.881, 95% CI: 0.845–0.918; Figure 3A). We further evaluated the value of CENPQ in the prognosis of HCC based on the grouping of cases by CENPQ median expression values. High expression of CENPQ was linked with worse OS (log-rank p = 0.002), DSS (log-rank p < 0.001), and PFI (log-rank p = 0.002), according to Kaplan-Meier survival curves (Figures 3B, C, and D). Further subgroup survival

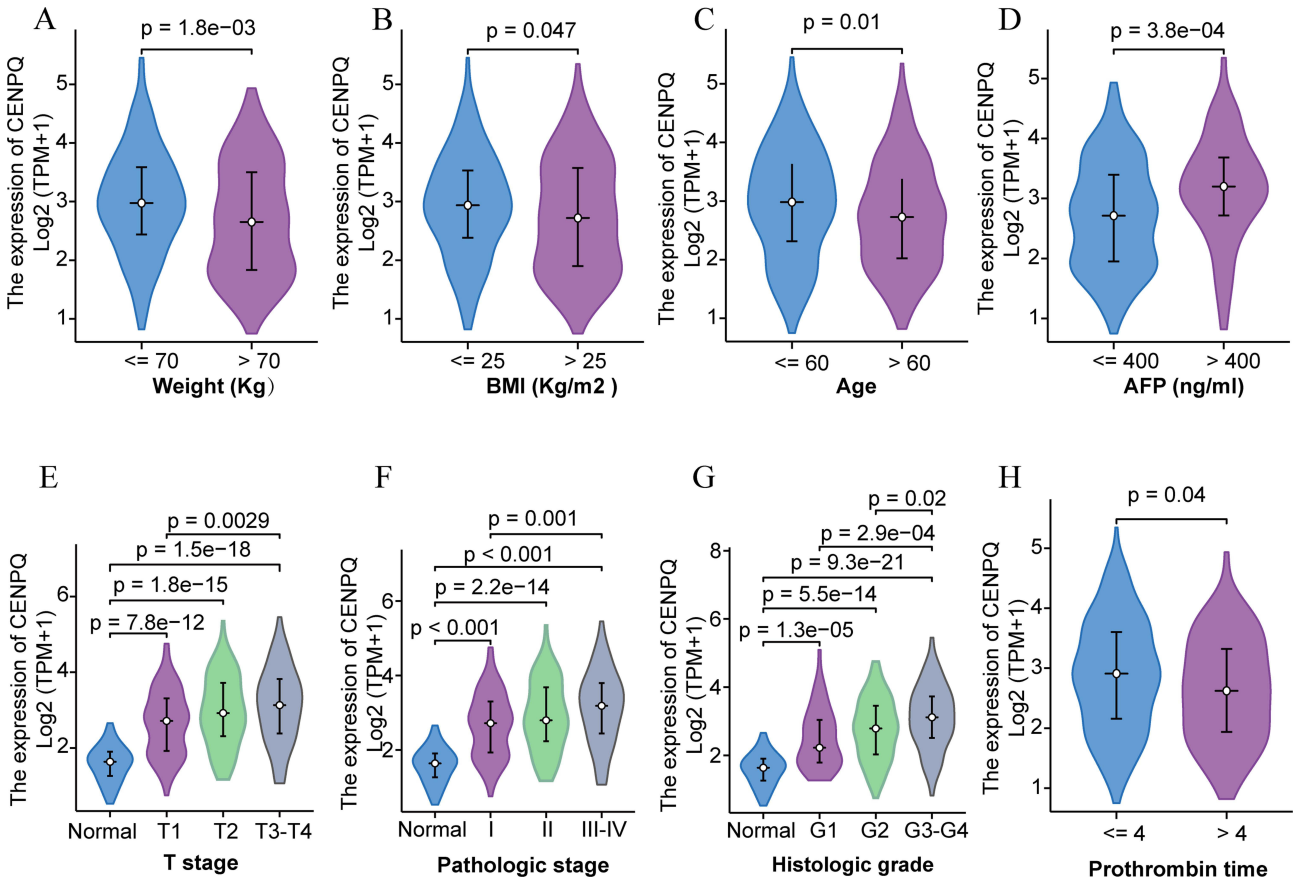

Figure 2 Correlation analysis of CENPQ expression and clinicopathological features in HCC. Violin plots summarizing CENPQ expression according to weight (**A**), BMI (**B**), age (**C**), AFP (**D**), T stage (**E**), pathologic stage (**F**), histological grade (**G**), and prothrombin time (**H**).
Abbreviations: BMI, body mass index; AFP, alpha fetoprotein; ALB, albumin.

Table 2 Correlation Between CENPQ Expression and Clinicopathological Features (Logistic Regression)

Characteristics	Cases	OR (95% CI)	P value
Gender (Male vs Female)	371	1.178 (0.763–1.822)	0.460
Age (years) (>60 vs ≤60)	370	0.555 (0.366–0.837)	**0.005**
Weight (kg) (>70 vs ≤70)	344	0.483 (0.313–0.741)	**< 0.001**
BMI (kg/□) (>25 vs ≤25)	335	0.643 (0.417–0.989)	**0.045**
AFP (ng/mL) (>400 vs ≤400)	278	3.243 (1.795–6.075)	**< 0.001**
ALB (g/dl) (≥3.5 vs <3.5)	297	1.669 (0.969–2.913)	0.067
Prothrombin time (sec) (>4 vs ≤4)	294	0.576 (0.345–0.954)	**0.033**
Child-Pugh grade (B-C vs A)	239	0.905 (0.368–2.186)	0.825
Ishak fibrosis score (3–6 vs 0–2)	212	1.167 (0.680–2.006)	0.576
T stage (T3-T4 vs T1-T2)	368	1.818 (1.130–2.957)	**0.015**
N stage (N1 vs N0)	256	2.727 (0.344–55.541)	0.388
M stage (M1 vs M0)	270	2.741 (0.346–55.799)	0.385
Pathologic stage (Stage III–IV vs Stage I–II)	347	2.035 (1.248–3.360)	**0.005**
Residual tumor (R1-R2 vs R0)	342	1.281 (0.493–3.435)	0.611
Histologic grade (G3-G4 vs G1-G2)	366	2.330 (1.510–3.626)	**< 0.001**
Adjacent hepatic tissue inflammation (Yes vs No)	234	1.071 (0.641–1.790)	0.794
Vascular invasion (Yes vs No)	315	1.382 (0.868–2.206)	0.173

Abbreviations: ALB, albumin; AFP, alpha fetoprotein; BMI, body mass index; CI, confidence interval; OR, odd ratio. Numbers in bold indicate significant differences at $p < 0.05$.

analysis revealed that high expression of CENPQ was associated with worse OS in the >60-year of age subgroup (log-rank p = 0.016; Figure 3E), in the ≤70 kg of weight subgroup (log-rank p < 0.001; Figure 3F), in the male subgroup (log-rank p = 0.004; Figure 3G), and in the T2-T4 stage subgroup (log-rank p = 0.016; Figure 3H). Further, univariate and multivariate analyses showed that CENPQ expression was an independent risk factor for OS (HR = 2.378, 95% CI = 1.122–5.039, p = 0.024; Figure 4A) and DSS (HR = 1.638, 95% CI = 1.053–2.547, p = 0.029; Figure 4B) in HCC patients. Further analysis showed that CENPQ expression was associated with worse PFI (HR = 1.586, 95% CI = 1.184–2.125, p = 0.002; Figure 4C), but it was not an independent risk factor for PFI in HCC patients.

Identification and Functional Enrichment Analysis of CENPQ-Associated DEGs

To assess potential biological roles of CENPQ in HCC, we identified DEGs in CENPQ high- and low-expression groups, determined from RNA-seq data in TCGA. This analysis revealed a total of 1506 DEGS, including 1142 up-regulated and 364 down-regulated genes (Figure 5A). GO analysis showed that these DEGs are mainly associated with Biological Processes (BP) such as regulation of mitotic cell cycle, organelle fission, and nuclear division (Figure 5B and Additional File Table S1). Several Cellular Component (CC) terms, centromeric region, chromosomal region, and DNA replication preinitiation complex, were also enriched by these DEGs (Figure 5B and Additional File Table S2). In the Molecular Function (MF) category, DEGs were mainly associated with the signaling receptor activator activity, receptor ligand activity, channel activity, and serine hydrolase activity terms (Figure 5B and Additional File Table S3). KEGG analysis indicated that cell cycle, complement and coagulation cascades, and bile secretion may be involved in CENPQ regulation of HCC (Figure 5B and Additional File Table S4). GSEA revealed a total of 40 pathways associated with differential CENPQ expression, including complement system, complement cascade, cell cycle, hippo-merlin signaling dysregulation, and degradation of the extracellular matrix (Figure 5C and D and Additional File Table S5). The above results suggest that CENPQ may be involved in the progression of HCC by influencing cell cycle, hippo-merlin signaling, and the complement system.

Correlation Analysis of CENPQ Expression and Immune Cell Infiltration

In the previous section, enrichment analyses suggested that CENPQ levels in HCC are associated with immune processes and factors such as complement system and complement cascade. Therefore, we analyzed the correlation between

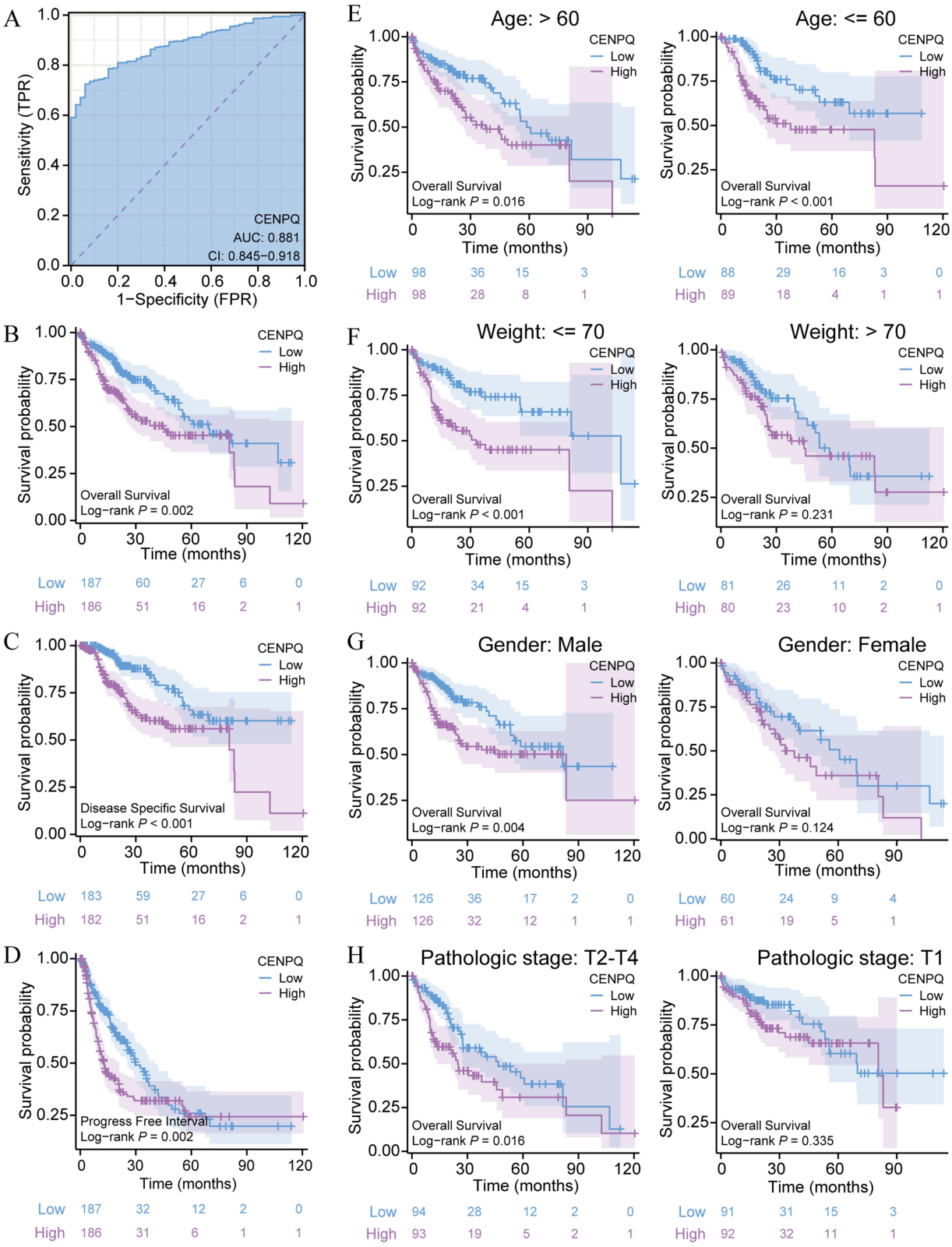

Figure 3 Diagnostic and prognostic value of CENPQ in HCC. (**A**) ROC analysis indicating good diagnostic performance of CENPQ mRNA profiling in distinguishing HCC samples from normal liver tissue. Kaplan-Meier curves showing the relationship between CENPQ expression and OS (**B**), DSS (**C**), and PFI (**D**). (**E–H**) Kaplan-Meier curves of OS in subgroups of HCC patients. (**E**) Age, >60 and ≤60 years, (**F**) weight, ≤70 and >70 kg, (**G**) gender, male and female, (**H**) pathological stage, T2-T4 and T1.
Abbreviations: AUC, area under the ROC curve; CI, 95% confidence interval; OS, overall survival; DSS, disease-specific survival; PFI, progression-free interval.

https://doi.org/10.2147/PGPM.S456965 DovePress

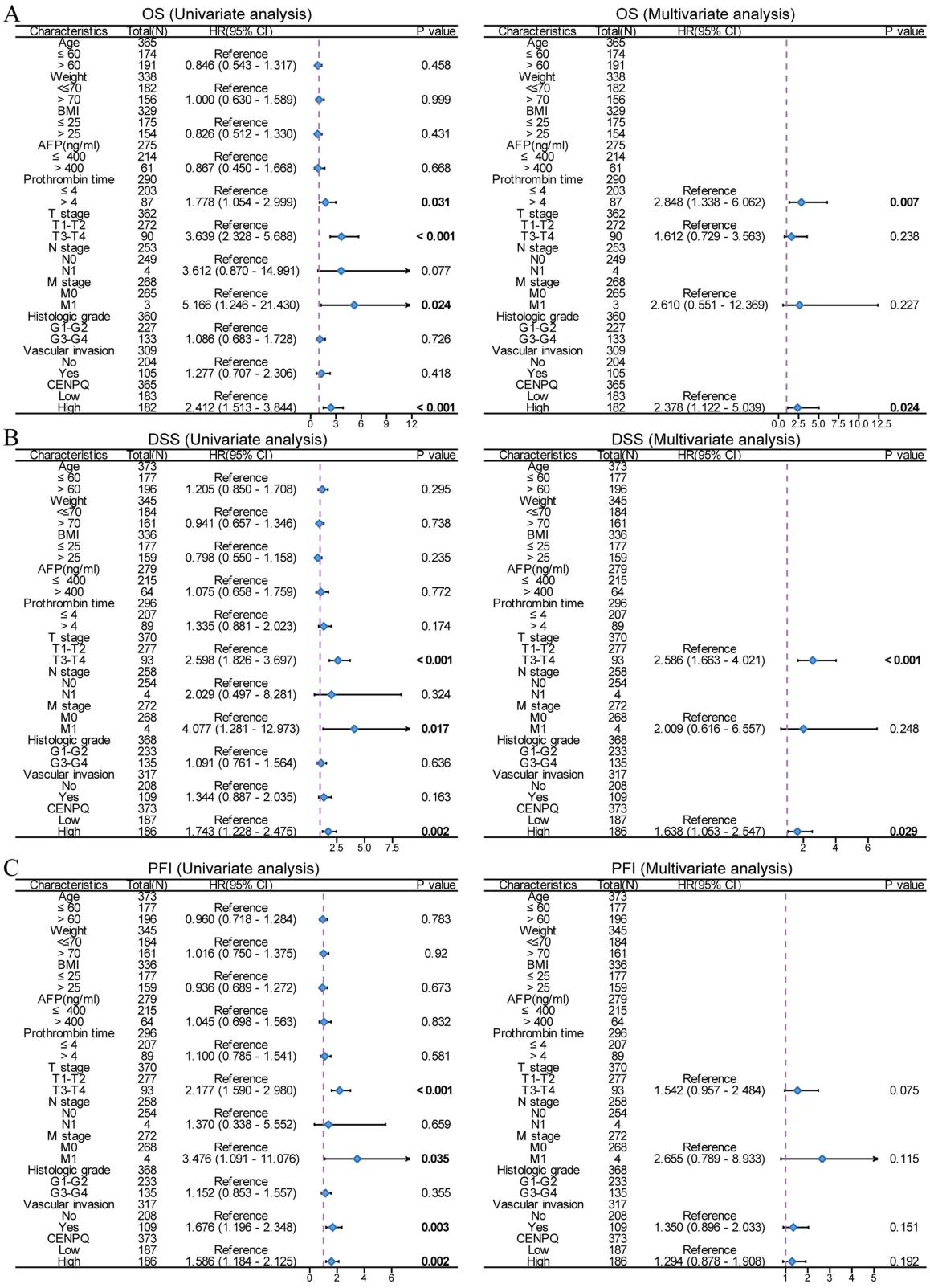

Figure 4 Univariate and multivariate Cox regression analyses of prognostic-related risk factors. Univariate and multivariate Cox regression analyses of risk factors associated with OS (**A**), DSS (**B**), and PFI (**C**) in HCC.

Abbreviations: OS, overall survival; DSS, disease-specific survival; PFI, progression-free interval.

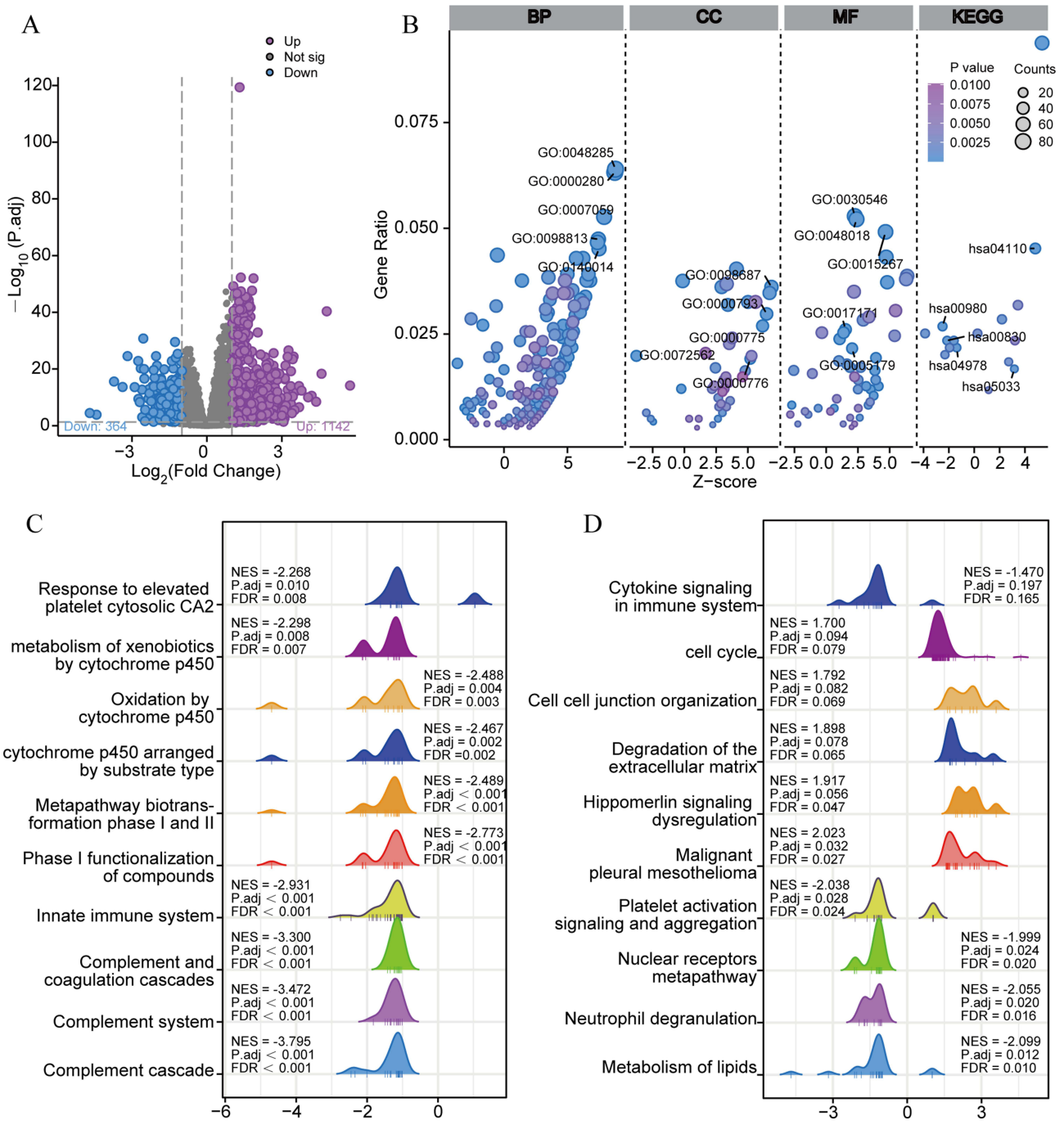

Figure 5 Identification of CENPQ-related DEGs in HCC and functional and pathway enrichment analyses. (**A**) Volcano plot of the distribution of DEGs. (**B**) BP, CC, MF, and KEGG terms for enrichment analysis of DEGs. (**C** and **D**) gene set enrichment analysis of DEGs.

Abbreviations: DEGs, differentially expressed genes; GO, gene ontology; BP, biological process; CC, cellular component; MF, molecular function; KEGG, Kyoto Encyclopedia of Genes and Genomes; NES, normalized enrichment score; FDR, false discovery rate.

CENPQ expression and immune infiltration in HCC. Interestingly, CENPQ expression was positively correlated with the expression of Th2 cells and 2 other types of immune cells, and negatively correlated with Th17 cells and 12 other types of immune cells (all $p < 0.05$; Figure 6A). The correlation between CENPQ and each of the 16 immune cell types analyzed was further evaluated separately. As shown in the chord diagram in Figure 6B, CENPQ was correlated to varying levels with distinct immune cells in HCC. The aforementioned findings prompted us to investigate the levels of immune cell infiltration in the CENPQ low and high expression groups. Infiltration scores for Th2 cells and T helper cells

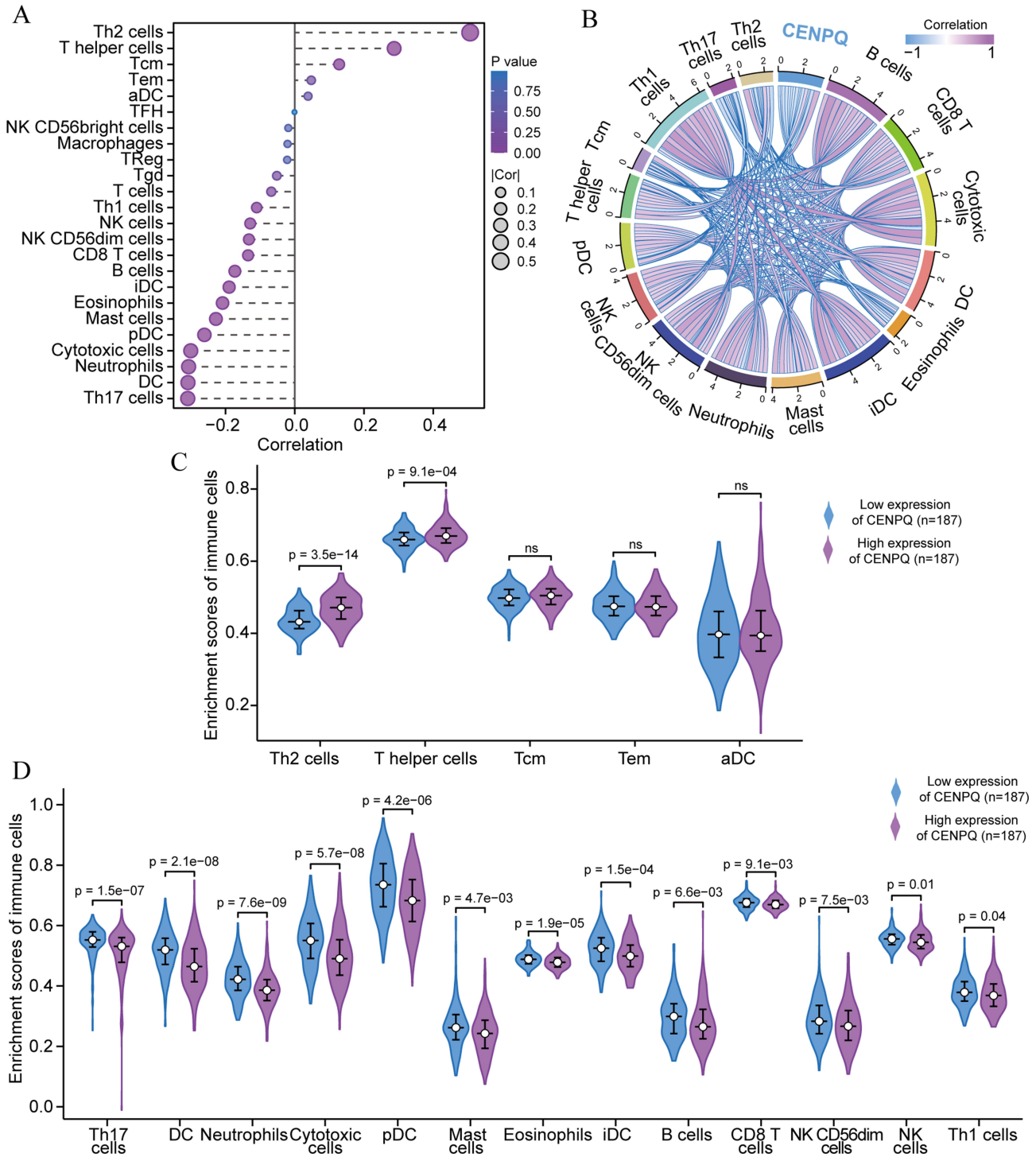

Figure 6 Correlation analysis of CENPQ expression and immune cell infiltration in HCC. (**A**) Correlation between CENPQ expression and the abundance of 24 tumor-infiltrating immune cell types. (**B**) Chord plot depicting the correlation between CENPQ and the abundance of 16 tumor-infiltrating immune cell types. Enrichment scores of positively correlated (**C**) and negatively correlated (**D**) immune cells in the CENPQ high and low expression groups.

Abbreviations: Treg, regulatory T cell; Tgd, gamma delta T cell; TFH, T follicular helper cell; Tem, T effector memory cell; DC, dendritic cell; pDC, plasmacytoid DC; NK cell, natural killer cell; iDC, immature DC; aDC, activated DC.

were higher in the CENPQ high expression group (Figure 6C), whereas infiltration scores for Th17 cells, DCs, neutrophils, cytotoxic cells, plasmacytoid dendritic cells (pDC), mast cells, eosinophils, immature DCs (iDCs), B cells, CD8 T cells, NK CD56^{dim} cells, NK cells, and Th1 cells were higher in the CENPQ low expression group

(Figure 6D). Furthermore, correlation analysis between CENPQ mRNA and classical immune checkpoints showed that CENPQ expression was positively correlated with PD-L1 (Spearman's r = 0.230; p < 0.001; Figure 7A), HAVCR2 (Spearman's r = 0.220; p < 0.001; Figure 7B), PD1 (Spearman's r = 0.211; p < 0.001; Figure 7C), CTLA4 (Spearman's r = 0.202; p < 0.001; Figure 7D), SIGLEC15 (Spearman's r = 0.147; p = 0.004; Figure 7E), PDCD1LG2 (Spearman's r = 0.121; p = 0.019; Figure 7F), LAG3 (Spearman's r = 0.205; p < 0.001; Figure 7G), and TIGIT (Spearman's r = 0.212; p < 0.001; Figure 7H). The heat map shown in Figure 7I summarizes correlation data between CENPQ and the above

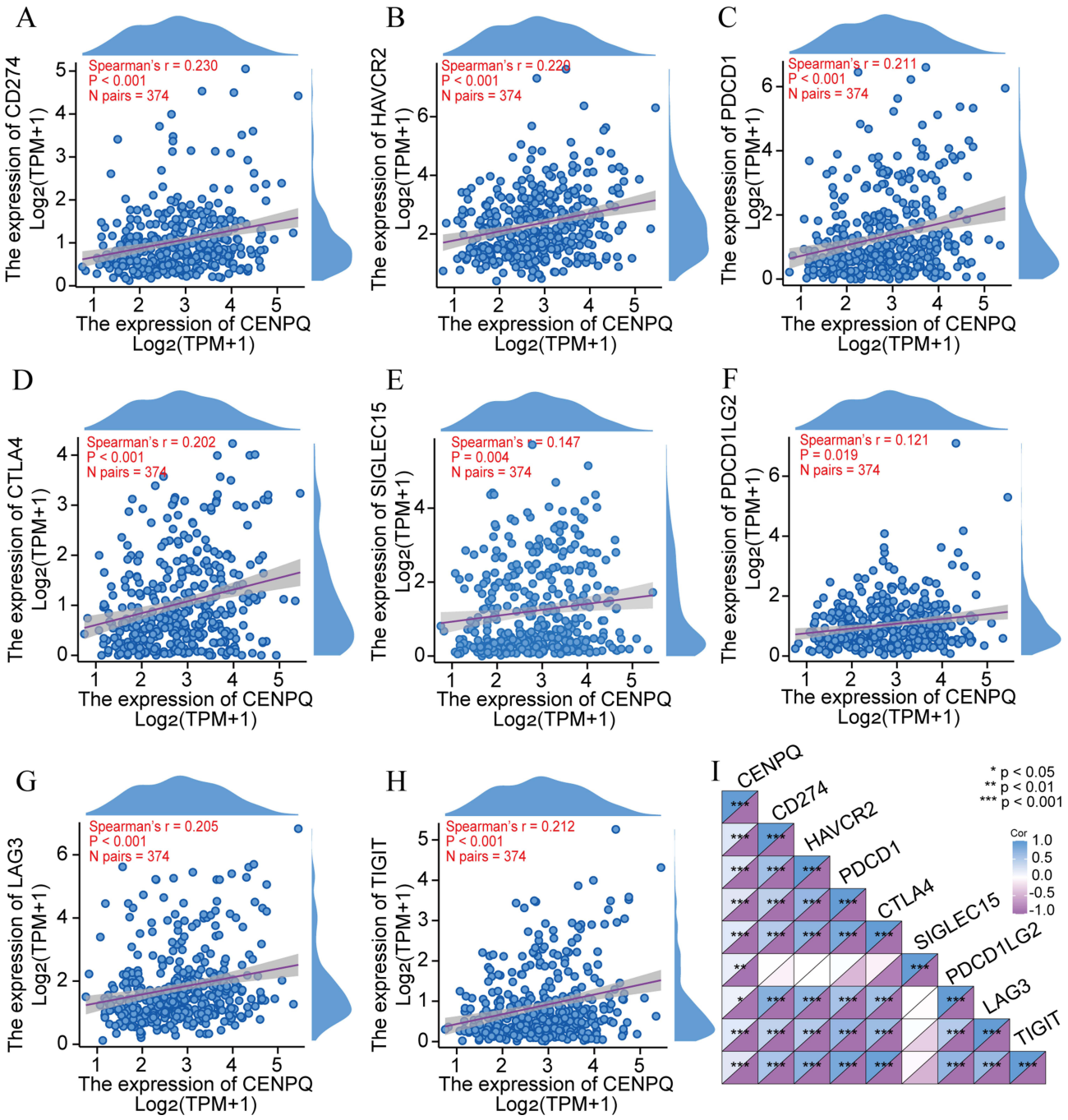

Figure 7 Correlation analysis of CENPQ expression and immune checkpoint genes in HCC. CENPQ was positively correlated with PD-L1 (**A**), HAVCR2 (**B**), PD1 (**C**), CTLA4 (**D**), SIGLEC15 (**E**), PDCD1LG2 (**F**), LAG3 (**G**) and TIGIT (**H**). (**I**) Heat map depicting the correlation of CENPQ with 8 immune checkpoint genes in HCC. *p < 0.05, **p < 0.01, ***p < 0.001.

immune checkpoints. These findings suggest that CENPQ may impact immunological tolerance in HCC immunotherapy by influencing the expression of various tumor immune checkpoints.

Validation of CENPQ Expression and Effects on Proliferation and Cycle of HCC Cells in vitro

Previous functional enrichment indicated that CENPQ is associated with cell cycle and nuclear division in HCC. Therefore, we next analyzed the correlation between CENPQ and cell cycle-dependent kinase family (CDK1, CDK2, CDK4, and CDK6) and cyclin family (CCNA, CCNB, CCNC, and CCNE). The results showed that up-regulated CENPQ in HCC was significantly positively correlated with cycle-dependent kinase (Figure 8A) and cyclin family (Figure 8B). To further confirm our bioinformatics results, we first examined through RT-qPCR the expression of CENPQ mRNA in 10 clinical HCC samples with matched normal liver specimens and four common HCC cell lines. Analysis of 10 pairs of clinical HCC and normal liver tissue samples showed that CENPQ mRNA expression was significantly increased in HCC (Figure 8C). CENPQ mRNA was relatively highly expressed in HUH7 and HEPG2 cells (Figure 8D). Therefore, we explored the function of CENPQ in HUH7 and HEPG2 cells. Firstly, three types of siRNA (siCENPQ-1, siCENPQ-2, and siCENPQ-3) and negative control siRNA (siNC) were designed to target the CENPQ gene sequence. The interference efficiency of the three siRNA and siNC with CENPQ in HUH7 and HEPG2 cells was examined by RT-PCR after transfection of siRNA and siNC. The results showed that siCENPQ-2 had the best interference efficiency in HUH7 (Figure 8E) and HEPG2 (Figure 8F), while siNC had no significant effect on CENPQ expression. Therefore, siCENPQ-2 was used as the siRNA interfering with CENPQ expression for subsequent experiments. Flow cytometry was performed to analyze the cell cycle. It showed that after interfering with the expression of CENPQ in HUH7 cells, the proportion of G0/G1 phase was increased and G2/M phase cells were decreased in the siCENPQ-2 group compared with the siNC group (Figure 8G). Similar results were obtained by cycle assay in HEPG2 cells (Figure 8H). The above results suggested that interfering with CENPQ caused HCC cells to arrest at the G0/G1 phase. Cell cycle alteration is usually closely associated with proliferation. We further examined the effect of CENPQ on HCC proliferation. CCK8 assay showed that the cell proliferation ability was significantly reduced in the siCENPQ-2 group compared to the siNC group (Figure 8I). Similar results were observed in HEPG2 cells (Figure 8J). These results suggested that interfering with CENPQ expression may inhibit the proliferation and arrest the cell cycle of HCC cells.

Discussion

Biomarkers and immunotherapeutic targets for the diagnosis and treatment of cancer have been studied extensively in recent years. Although immune checkpoint blockers have been shown to improve the prognosis of patients with advanced HCC, recent statistics point that the general outcome of patients with HCC remains unsatisfactory.[24] Therefore, the search for new diagnostic and prognostic markers and effective therapeutic targets is important to improve the prognosis of HCC patients and the development of therapeutic drugs.

The CENPQ gene family plays an important role in controlling mitotic chromosome segregation and shows tightly controlled expression patterns in cells.[25] In recent years, numerous studies have shown that abnormal expression of CENP family members influences the development of various cancers. For example, CENPN affects the proliferation, cell cycle, and glucose metabolism of nasopharyngeal carcinoma cells via the AKT signaling pathway.[26] Studies indicated that CENPK promotes the epithelial-mesenchymal transition of liver cancer cells by decreasing N-cadherin and activating E-cadherin expression.[27] In renal cell carcinoma, CENPA promotes cancer cell metastasis by activating the Wnt/β-catenin signaling pathway.[28] In breast cancer, CENPQ is regulated by LINC01857 and miR-2052 to induce cancer cell metastasis and angiogenesis.[18] However, according to our knowledge, no study has reported on the role of CENPQ in HCC. Our pan-cancer analysis indicated that CENPQ expression was upregulated in most cancers, suggesting the broad applicability of CENPQ screening in cancer identification. In contrast, suggestive of tumor-specific expression patterns, CENPQ expression was decreased in acute myeloid leukemia. We integrated multiple databases to analyze the expression of CENPQ in HCC, and detected upregulated expression, at both mRNA and protein levels, in HCC compared to normal liver. We also confirmed its overexpression in clinical HCC samples relative to matched normal liver tissue specimens by

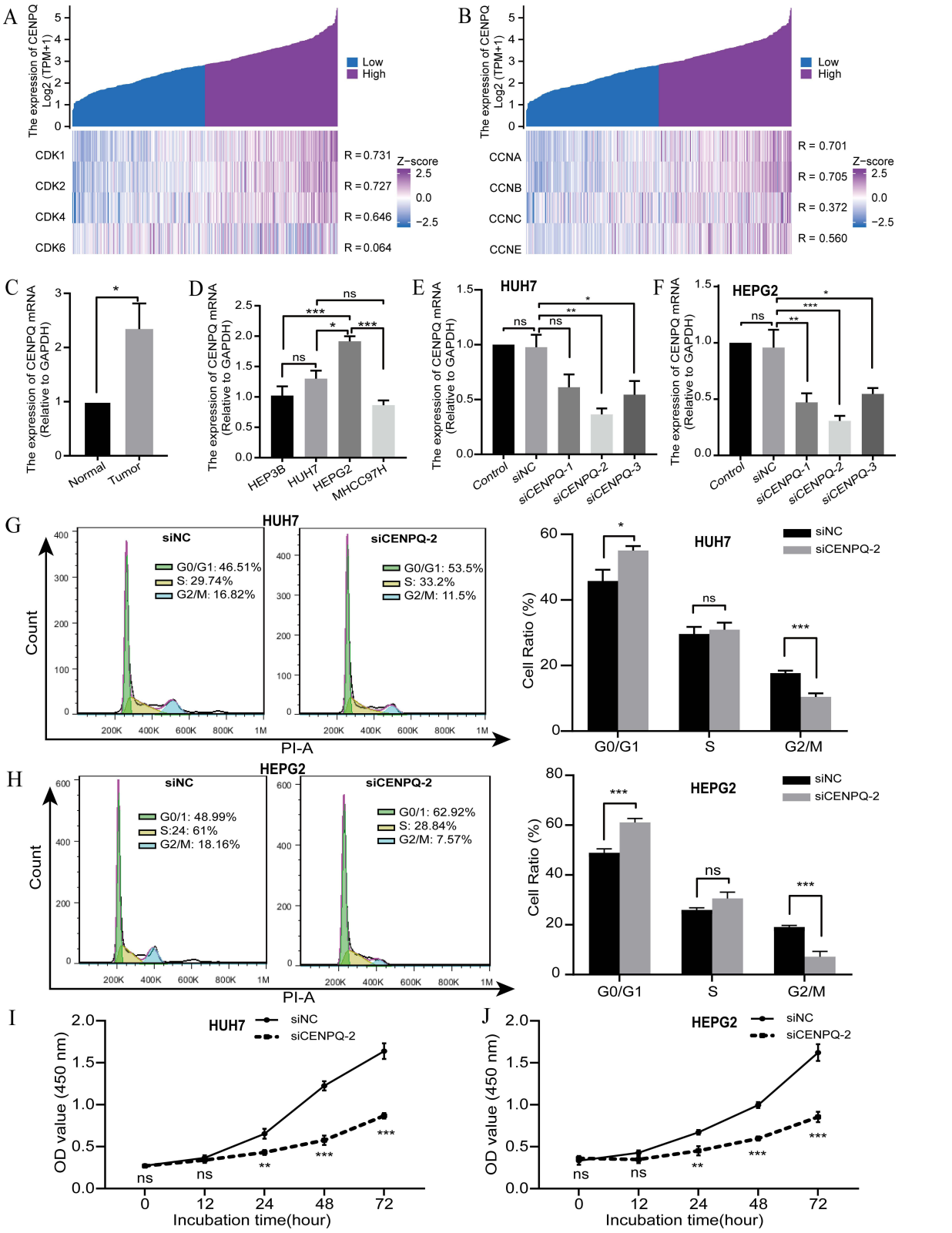

Figure 8 CENPQ is involved in the regulation of HCC cell cycle and proliferation. (**A**) Heatmap of the correlation between CENPQ and CDK gene family (CDK1, CDK2, CDK4, CDK6). (**B**) Heatmap of the correlation between the expression of CENPQ and CCNA, CCNB, CCNC, and CCNE. (**C**) Expression of CENPQ mRNA in HCC and normal liver tissues. (**D**) Expression of CENPQ mRNA in HCC cell lines. Silencing of CENPQ in HCC cell lines HUH7 (**E**) and HEPG2 (**F**). Flow cytometry was used to detect cycle changes in HUH7 (**G**) and HEPG2 (**H**). CCK-8 was used to detect viability changes of HUH7 (**I**) and HEPG2 (**J**).*p < 0.05, **p < 0.01, ***p < 0.001.

https://doi.org/10.2147/PGPM.S456965 DovePress

RT-qPCR. Of note, ROC analysis indicated that CENPQ might be a promising diagnostic indicator for HCC, whereas high expression of CENPQ was associated with poor prognosis (OS, DSS, and PFI) in HCC patients. These studies thus suggest that CENPQ may be a potential diagnostic and prognostic marker in HCC.

The analysis of tumor-associated DEGs is useful to unmask potentially relevant structural or functional associations for specific target genes. Based on functional and pathway enrichment analyses of 1506 CENPQ-related DEGs identified in the TCGA database, we revealed significant enrichment for these DEGs in biological processes such as regulation of mitotic cell cycle, meiotic cell cycle, mitotic nuclear division, and mitotic cell cycle phase transition. GSEA further showed that the innate immune system, cell cycle, complement system, and cell-cell junction organization, among other signaling pathways, were significantly enriched in the DEGs. Co-expression analysis showed a significant positive correlation between CENPQ and cell cycle-dependent kinase family (CDK1/CDK2/CDK4/CDK6), and cell cyclin family (CCNA/CCNB/CCNC/CCNE). Recent studies have revealed that the CENP family plays a crucial role in the cell cycle progression of cancer. The proportion of cells in the G0/G1 phase was significantly reduced after knockdown of the CENPM in HCC cells.[29] In HUH7 and HEPG2 cells, down-regulation of CENPN expression inhibited the transition from G1 to S phase.[30] In HCC cells HUH7 and MHCC97H, knockdown of CENPU caused cell cycle arrest in the G0/G1 phase, while CDK2, CDK4, CDK6, cyclin D1, and cyclin E1 were significantly downregulated.[31] Knockdown of CENPW in HCC cells BEL-7402 and HEPG2 increased the proportion of G0/G1 phase cells and decreased the proportion of S phase cells.[17] We further demonstrated that interfering with CENPQ in HCC may affect HCC cell cycle processes in vitro. We found cell cycle arrest in the G0/G1 phase and reduced cell viability after the knockdown of CENPQ in HCC cells HUH7 and HEPG2. These studies suggest that the aberrantly expressed CENP family, including CENPQ, plays an essential role in the cell cycle process of HCC progression. Although more detailed studies are warranted, these preliminary findings would suggest that the cell cycle pathway is impacted by dysregulated CENPQ expression in HCC.

Systemic therapy combined with immunotherapy has become one of the standard treatment options for patients with advanced HCC. Several recent studies have shown that the level of immune cell infiltration in the tumor microenvironment can influence the efficacy of immunotherapy.[32,33] The tumor microenvironment contains numerous immune cells such as T-cells, B-cells, Th2-cells, neutrophils, and DC-cells.[34] However, the relationship between CENPQ and immune infiltrating cells in HCC has been less studied. Our study assessed the relationship between CENPQ expression in HCC and the abundance of infiltrating immune cell subpopulations based on the ssGSEA algorithm. The results revealed that CENPQ expression was associated with multiple immune cell subsets, with the most pronounced positive correlation noted for Th2 cells and the most negative correlation for Th17 cells. As an inflammation-associated tumor, the imbalance between pro-inflammatory Th1 cells and anti-inflammatory Th2 cells plays an important role in HCC metastasis.[35] It has been shown that Th2 cells can induce macrophage polarization from M1 to M2 status, with immunosuppressive and pro-tumorigenic activities.[36] Hence, higher Th2 levels in CENPQ-overexpressing tumors might contribute to decreased immune cytotoxicity. Recent studies have described new immunogenomic profiles that classify HCC into inflamed and non-inflamed classes of HCC, which show different sensitivities to immunotherapeutic responses.[37] In inflamed HCC, the tumor microenvironment in which tumor cells coordinate inflammation is often accompanied by myeloid cell infiltration.[38] Disproportionate myeloid cell infiltration may lead to a shift in the balance of myeloid responses from antitumor to tumor activity.[39] We found that neutrophils differed between low- and high-CENPQ HCC tissues. This suggests that CENPQ may influence the HCC immune microenvironment by altering the levels of neutrophils in HCC. Our current analysis may thus suggest that CENPQ levels may affect immune cell profiles in HCC to regulate tumor immunity. Furthermore, there was a significant positive association between CENPQ expression and some immunological checkpoints [CD274 (PD-L1), HAVCR2, PDCD1 (PD1), CTLA4, SIGLEC15, PDCD1LG2, LAG3, and TIGIT]. These results suggested that CENPQ overexpression may affect HCC by regulating the levels of infiltrating immune cells.

In conclusion, we reported for the first time that high CENPQ expression is positively associated with poor prognosis in HCC, and highlighted also potentially relevant associations between CENPQ expression and immune infiltration and cell cycle. Our work provides multi-level evidence for the potential of CENPQ in HCC as a biomarker. Meanwhile, we identified CENPQ as a crucial regulator in HCC proliferation and cell cycle progression. Our study has some limitations.

First, as this study was mainly based on analysis of public databases, validation against large clinical cohorts is necessary to verify CENPQ mRNA/protein expression data, as well as its usefulness as a diagnostic and prognostic marker for HCC. Second, in vivo, experiments in animal models are needed to confirm the mechanism by which CENPQ may contribute to poor prognosis. In summary, although more specific studies are clearly needed, our study suggests that CENPQ may represent a novel biomarker and potential immunotherapeutic target for HCC.

Funding

This work was supported by the National Health Care Commission (Grant No. WA2021RW26) and the Science and Technology Development Program of the Affiliated Hospital of North Sichuan Medical College (Grant No. 2019ZX001).

Disclosure

Kun He, Meng-yi Xie and Xiao-jin Gao are co-first authors for this study. The authors report no conflicts of interest in this work.

References

1. Affo S, Yu LX, Schwabe RF. The role of cancer-associated fibroblasts and fibrosis in liver cancer. *Ann Revi Pathol*. 2017;12(153–186):153–186. doi:10.1146/annurev-pathol-052016-100322
2. Vogel A, Cervantes A, Chau I, et al. Hepatocellular carcinoma: ESMO clinical practice guidelines for diagnosis, treatment and follow-up. *Ann Oncol*. 2018;29(Suppl 4):iv238–iv255. doi:10.1093/annonc/mdy308
3. Thomas MB, Jaffe D, Choti MM, et al. Hepatocellular carcinoma: consensus recommendations of the national cancer institute clinical trials planning meeting. *J Clin Oncol*. 2010;28(25):3994–4005. doi:10.1200/JCO.2010.28.7805
4. Sangro B, Gomez-Martin C, De La Mata M, et al. A clinical trial of CTLA-4 blockade with tremelimumab in patients with hepatocellular carcinoma and chronic hepatitis C. *J Hepatol*. 2013;59(1):81–88. doi:10.1016/j.jhep.2013.02.022
5. El-Khoueiry AB, Sangro B, Yau T, et al. Nivolumab in patients with advanced hepatocellular carcinoma (CheckMate 040): an open-label, non-comparative, Phase 1/2 dose escalation and expansion trial. *Lancet*. 2017;389(10088):2492–2502. doi:10.1016/S0140-6736(17)31046-2
6. Zhu AX, Finn RS, Edeline J, et al. Pembrolizumab in patients with advanced hepatocellular carcinoma previously treated with sorafenib (KEYNOTE-224): a non-randomised, open-label Phase 2 trial. *Lancet Oncol*. 2018;19(7):940–952. doi:10.1016/S1470-2045(18)30351-6
7. El-Serag HB. Hepatocellular carcinoma. *N Engl J Med*. 2011;365(12):1118–1127. doi:10.1056/NEJMra1001683
8. Banales JM, Marin JJG, Lamarca A, et al. Cholangiocarcinoma 2020: the next horizon in mechanisms and management. *Nat Rev Gastroenterol Hepatol*. 2020;17(9):557–588. doi:10.1038/s41575-020-0310-z
9. Johnson SC, Mcclelland SE. Watching cancer cells evolve through chromosomal instability. *Nature*. 2019;570(7760):166–167. doi:10.1038/d41586-019-01709-2
10. Liu Y, Xiong S, Liu S, et al. Analysis of gene expression in bladder cancer: possible involvement of mitosis and complement and coagulation cascades signaling pathway. *J Comput Biol*. 2020;27(6):987–998. doi:10.1089/cmb.2019.0237
11. Liu Z, Chen C, Yan M, et al. CENPO regulated proliferation and apoptosis of colorectal cancer in a p53-dependent manner. *Discover Oncol*. 2022;13(1):8. doi:10.1007/s12672-022-00469-2
12. Y CAO, XIONG J, LI Z, et al. CENPO expression regulates gastric cancer cell proliferation and is associated with poor patient prognosis. *Molecu Med Rep*. 2019;20(4):3661–3670. doi:10.3892/mmr.2019.10624
13. He P, Hu P, Yang C, et al. Reduced expression of CENP-E contributes to the development of hepatocellular carcinoma and is associated with adverse clinical features. *Biomed Pharmacother*. 2020;123:109795. doi:10.1016/j.biopha.2019.109795
14. Huang Y, Chen X, Wang L, et al. Centromere Protein F (CENPF) serves as a potential prognostic biomarker and target for human hepatocellular carcinoma. *J Cancer*. 2021;12(10):2933–2951. doi:10.7150/jca.52187
15. Lu G, Hou H, Lu X, et al. CENP-H regulates the cell growth of human hepatocellular carcinoma cells through the mitochondrial apoptotic pathway. *Oncol Rep*. 2017;37(6):3484–3492. doi:10.3892/or.2017.5602
16. He K, Xie M, Li J, et al. CENPO is associated with immune cell infiltration and is a potential diagnostic and prognostic marker for hepatocellular carcinoma. *Int J Gen Med*. 2022;15:7493–7510. doi:10.2147/IJGM.S382234
17. Zhou Y, Chai H, Guo L, et al. Knockdown of CENPW inhibits hepatocellular carcinoma progression by inactivating E2F signaling. *Technol Cancer Res Treat*. 2021;20:15330338211007253. doi:10.1177/15330338211007253
18. Qian W, Yang L, Ni Y, et al. LncRNA LINC01857 reduces metastasis and angiogenesis in breast cancer cells via regulating miR-2052/CENPQ axis. *Open Med*. 2022;17(1):1357–1367. doi:10.1515/med-2022-0525
19. Diaz G, Engle RE, Tice A, et al. Molecular signature and mechanisms of hepatitis D virus-associated hepatocellular carcinoma. *Mol Cancer Res*. 2018;16(9):1406–1419. doi:10.1158/1541-7786.MCR-18-0012
20. Uhlén M, Fagerberg L, Hallström BM, et al. Proteomics. Tissue-based map of the human proteome. *Science*. 2015;347(6220):1260419. doi:10.1126/science.1260419
21. Love MI, Huber W, Anders S. Moderated estimation of fold change and dispersion for RNA-seq data with DESeq2. *Genome Biol*. 2014;15(12):550. doi:10.1186/s13059-014-0550-8
22. Yu G, Wang LG, Han Y, et al. clusterProfiler: an R package for comparing biological themes among gene clusters. *Omics*. 2012;16(5):284–287. doi:10.1089/omi.2011.0118
23. Hänzelmann S, Castelo R, Guinney J. GSVA: gene set variation analysis for microarray and RNA-seq data. *BMC Bioinf*. 2013;14(1):7. doi:10.1186/1471-2105-14-7

24. Sung H, Ferlay J, Siegel RL, et al. Global cancer statistics 2020: GLOBOCAN estimates of incidence and mortality worldwide for 36 cancers in 185 countries. *CA*. 2021;71(3):209–249. doi:10.3322/caac.21660
25. Perpelescu M, Fukagawa T. The ABCs of CENPs. *Chromosoma*. 2011;120(5):425–446. doi:10.1007/s00412-011-0330-0
26. Qi CL, Huang ML, Zou Y, et al. The IRF2/CENP-N/AKT signaling axis promotes proliferation, cell cycling and apoptosis resistance in nasopharyngeal carcinoma cells by increasing aerobic glycolysis. *J Exp Clin Cancer Res*. 2021;40(1):390. doi:10.1186/s13046-021-02191-3
27. Wang J, Li H, Xia C, et al. Downregulation of CENPK suppresses hepatocellular carcinoma malignant progression through regulating YAP1. *Onco Targets Ther*. 2019;12(869–882):1.
28. Takahashi Y, Tanikawa C, Miyamoto T, et al. Regulation of tubular recycling endosome biogenesis by the p53-MICALL1 pathway. *Int j Oncol*. 2017;51(2):724–736. doi:10.3892/ijo.2017.4060
29. Xiao Y, Najeeb RM, Ma D, et al. Upregulation of CENPM promotes hepatocarcinogenesis through mutiple mechanisms. *J Exp Clin Cancer Res*. 2019;38(1):458. doi:10.1186/s13046-019-1444-0
30. Wang Q, Yu X, Zheng Z, et al. Centromere protein N may be a novel malignant prognostic biomarker for hepatocellular carcinoma. *PeerJ*. 2021;9:e11342. doi:10.7717/peerj.11342
31. Liu Y, Yao Y, Liao B, et al. A positive feedback loop of CENPU/E2F6/E2F1 facilitates proliferation and metastasis via ubiquitination of E2F6 in hepatocellular carcinoma. *Int J Biol Sci*. 2022;18(10):4071–4087. doi:10.7150/ijbs.69495
32. Fridman WH, Pagès F, Sautès-Fridman C, et al. The immune contexture in human tumours: impact on clinical outcome. *Nat Rev Cancer*. 2012;12(4):298–306. doi:10.1038/nrc3245
33. Zhang H, Liu H, Shen Z, et al. Tumor-infiltrating neutrophils is prognostic and predictive for postoperative adjuvant chemotherapy benefit in patients with gastric cancer. *Ann Surg*. 2018;267(2):311–318. doi:10.1097/SLA.0000000000002058
34. Lei X, Lei Y, Li JK, et al. Immune cells within the tumor microenvironment: biological functions and roles in cancer immunotherapy. *Cancer Lett*. 2020;470:126–133. doi:10.1016/j.canlet.2019.11.009
35. Budhu A, Wang XW. The role of cytokines in hepatocellular carcinoma. *J Leukoc Biol*. 2006;80(6):1197–1213. doi:10.1189/jlb.0506297
36. Denardo DG, Barreto JB, Andreu P, et al. CD4(+) T cells regulate pulmonary metastasis of mammary carcinomas by enhancing protumor properties of macrophages. *Cancer Cell*. 2009;16(2):91–102. doi:10.1016/j.ccr.2009.06.018
37. Montironi C, Castet F, Haber PK, et al. Inflamed and non-inflamed classes of HCC: a revised immunogenomic classification. *Gut*. 2023;72(1):129–140. doi:10.1136/gutjnl-2021-325918
38. Fu Y, Mackowiak B, Feng D, et al. MicroRNA-223 attenuates hepatocarcinogenesis by blocking hypoxia-driven angiogenesis and immunosuppression. *Gut*. 2023;72(10):1942–1958. doi:10.1136/gutjnl-2022-327924
39. Wu C, Lin J, Weng Y, et al. Myeloid signature reveals immune contexture and predicts the prognosis of hepatocellular carcinoma. *J Clin Invest*. 2020;130(9):4679–4693. doi:10.1172/JCI135048